3D Bioprinted Human Liver Tissue for Modeling Progressive Liver Disease

Alice E. Chen[1], Dwayne Carter[1], Candace C. Grundy[1], Rhiannon N. Hardwick[1], Jeffrey T. Irelan[1], Leah M. Norona[2,3], Sharon C. Presnell[1], Deborah G. Nguyen[1]
[1]Organovo, Inc., San Diego, CA; [2]University of North Carolina at Chapel Hill, Chapel Hill, NC; [3]Institute for Drug Safety Sciences, Research Triangle Park, NC

Abstract

Translation of preclinical data to clinical outcomes remains an ongoing challenge in drug development. 3D bioprinted tissues exhibiting physiological tissue-like responses can be created to bridge this gap, through spatially-controlled, automated deposition of tissue-specific cell types. These multicellular, human *in vitro* tissue models enable improved cellular interactions and assessment of biological responses at the biochemical, genomic, and histological levels over extended time in culture. Organovo's ExVive™ Human Liver can be used to model chronic liver disease relevant phenotypes including steatosis, inflammation, and fibrosis. Incorporation of Kupffer cells and stimulation with inflammatory signals induces inflammatory cytokine release. Chronic exposure to drugs known to induce steatosis such as valproic acid, or to nutrient overload (free fatty acids) induces formation of lipid droplets. Chronic exposure to chemical inducers of fibrosis or TGFβ stimulation leads to stellate cell activation and fibrosis. Finally, inflammatory inducers and nutrient overload together lead to steatosis and fibrosis. These results suggest that ExVive™ Human Liver Tissue holds promise for the study of complex, chronic conditions such as NASH, enabling the discovery of novel therapeutics, biomarkers, and safety assessment of drugs in a disease-relevant background.

Technology Overview

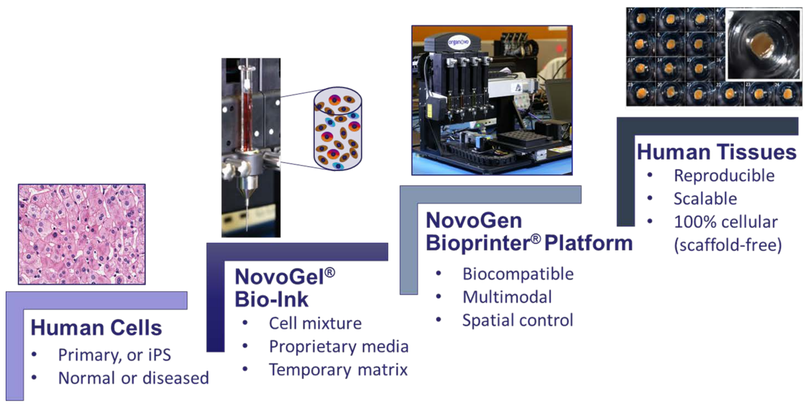

Figure 1: 3D human tissue development using the NovoGen Bioprinter® Platform**.** Cells reside in heterogeneous and architecturally structured 3D environments *in vivo.* Using the proprietary NovoGen Bioprinter® Platform, Organovo builds 3D tissues through automated, spatially-controlled cellular deposition to better recapitulate native tissue structure and function.

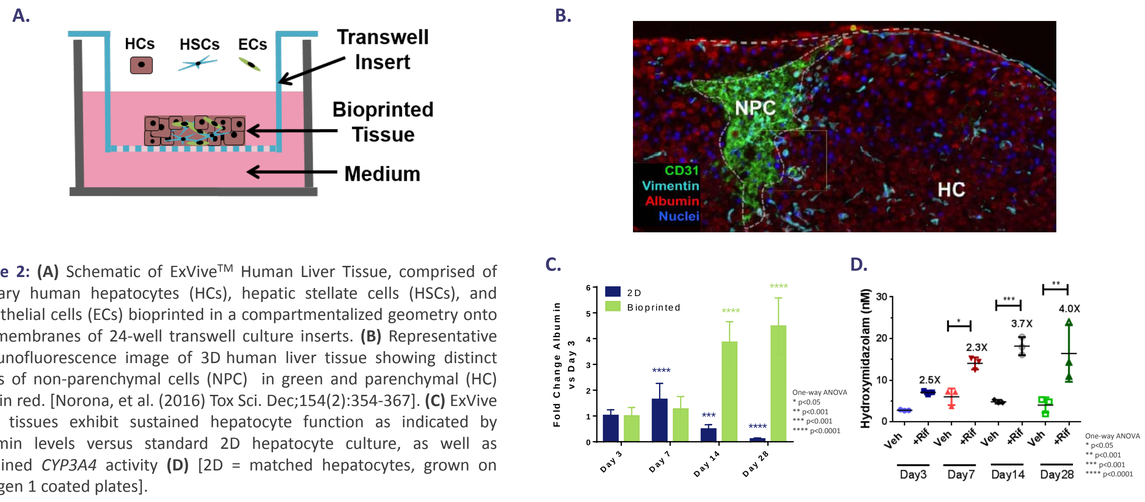

Figure 2: (A) Schematic of ExVive™ Human Liver Tissue, comprised of primary human hepatocytes (HCs), hepatic stellate cells (HSCs), and endothelial cells (ECs) bioprinted in a compartmentalized geometry onto the membranes of 24-well transwell culture inserts. **(B)** Representative immunofluorescence image of 3D human liver tissue showing distinct zones of non-parenchymal cells (NPC) in green and parenchymal (HC) cells in red. [Norona, et al. (2016) Tox Sci. Dec;154(2):354-367]. **(C)** ExVive Liver tissues exhibit sustained hepatocyte function as indicated by albumin levels versus standard 2D hepatocyte culture, as well as sustained *CYP3A4* activity **(D)** [2D = matched hepatocytes, grown on collagen 1 coated plates].

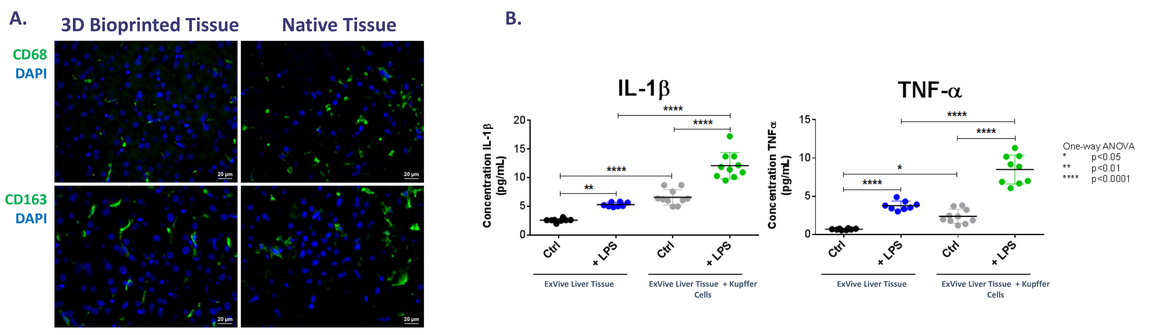

Figure 3: Characterization of bioprinted liver tissue with incorporation of Kupffer cells. **(A)** Kupffer cells in bioprinted liver express prototypical markers such as CD68 and CD168, and a staining pattern similar to native liver. **(B)** ExVive™ Liver Tissue with Kupffer cells exhibited greater cytokine induction after lipopolysaccharide (LPS) treatment. Media samples from tissue treated with LPS (100 µg/mL for 24h) were analyzed via electrochemiluminesce.

Drug and Nutrient Induced Steatosis in ExVive™ Human Liver Tissue

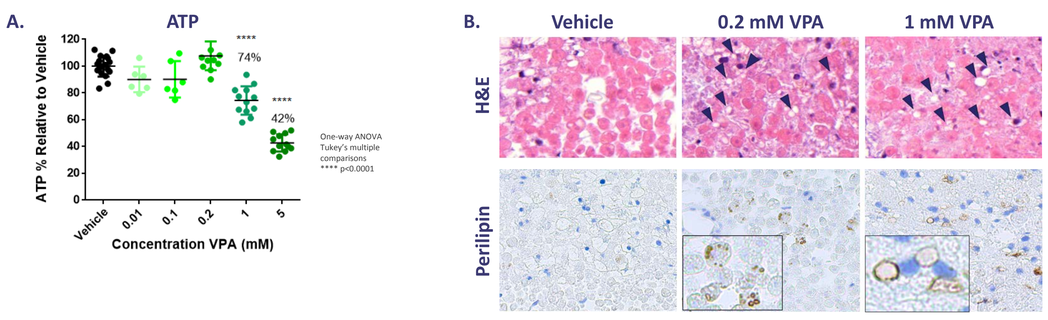

Figure 4: Valproic acid (VPA) is prescribed for epilepsy, bipolar disorder and migraine; ~5% of patients develop ALT elevations, usually asymptomatic or resolving but rarer, severe injury occurs with mitochondrial toxicity and steatosis. **(A)** Viability of 3D bioprinted liver tissue declines with increasing dose of VPA. **(B)** H&E staining of VPA treated tissues shows a vesicular steatotic phenotype (arrowheads). Perilipin (PLN5) staining of lipid vesicles further confirms the steatotic phenotype.

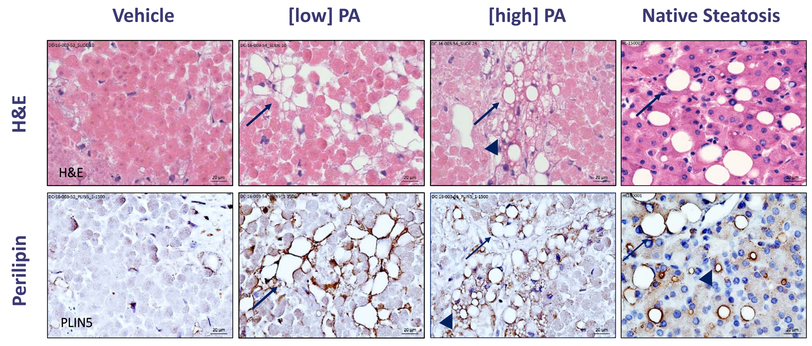

Figure 5: Palmitic acid (PA)-treated tissues exhibit increased incidence of putative lipid vesicles. H&E staining of PA treated tissues shows both macro- (arrows) and micro- (arrowheads) vesicular phenotypes. Perilipin (PLN5) staining of lipid vesicles further confirms the steatotic phenotype.

Induced Stellate Cell Activation and Fibrosis in ExVive™ Liver Tissue

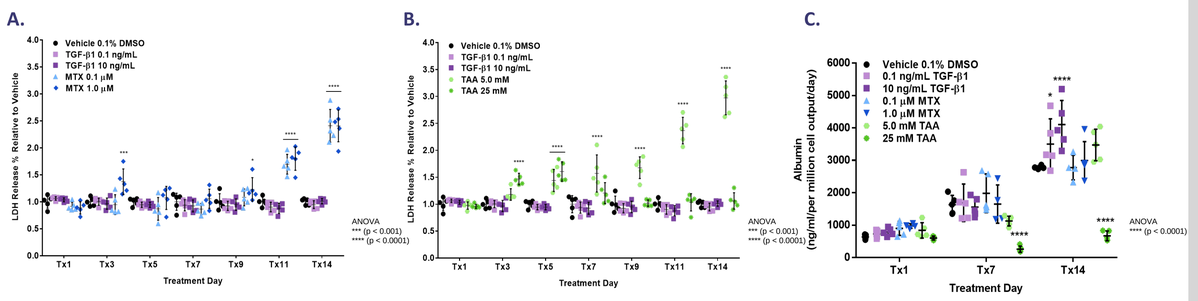

Figure 6: Impact of fibrotic agents on bioprinted liver tissue viability and functionality. 14-day treatment with MTX **(A)** and TAA **(B)** resulted in tissue damage, as evidenced by significant increases in LDH release (n = 9 for Tx1-Tx7, n = 5 for Tx9-Tx14) . Conversely, no overt damage is observed with TGFβ treatment. The degree of hepatocellular damage as measured by albumin output (**C**; n = 5) at key time points during the treatment period was most pronounced with 25 mM TAA, as demonstrated by a statistically significant decrease in albumin output relative to vehicle treated control.

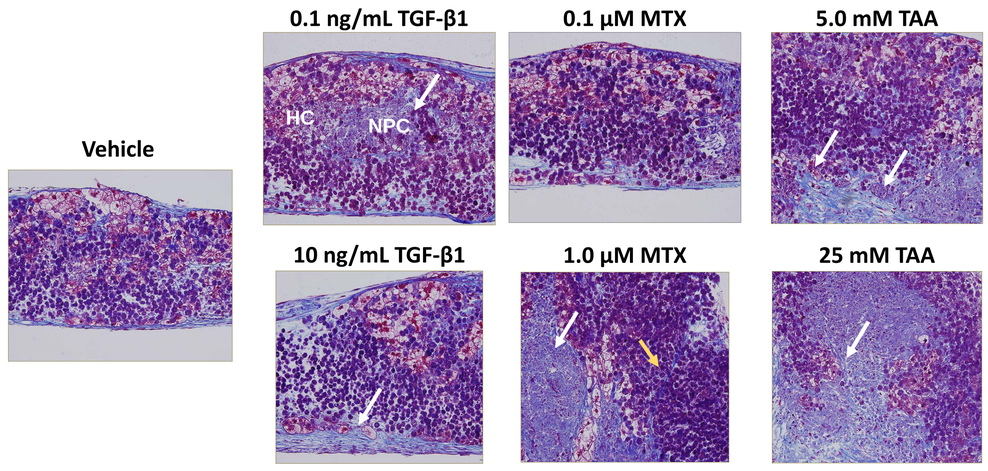

Figure 7: Histological assessment of bioprinted liver treated with fibrotic agents. Fixed tissues sections were stained with Gomori's One-Step trichrome to visualize collagen (blue), cytoplasm (pink/purple), and nuclei (dark purple). TGF-β1 treatment caused focal nodular fibrosis (white arrows) in the nonparenchymal compartment (NPC) but generally preserved hepatocellular (HC) mass. MTX caused mild hepatocellular damage and nodular and pericellular fibrosis at lower doses, with evidence of bridging fibrosis (yellow arrow) connecting NPC at 1.0 µM. Treatment with TAA nearly eliminated HCs in the tissues by 14 days, with the majority of tissue replaced by fibrotic scar tissue.

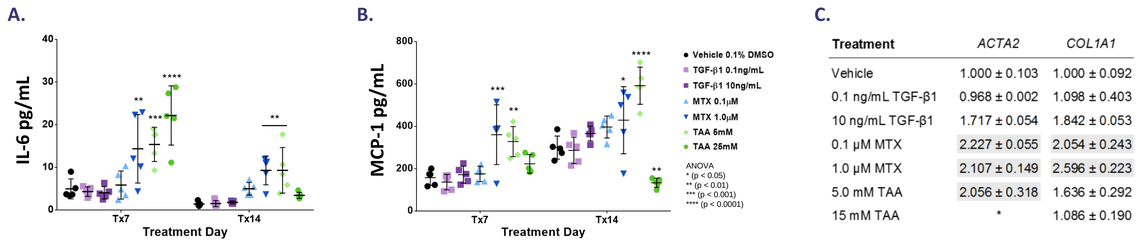

Treatment	*ACTA2*	*COL1A1*
Vehicle	1.000 ± 0.103	1.000 ± 0.092
0.1 ng/mL TGF-β1	0.968 ± 0.002	1.098 ± 0.403
10 ng/mL TGF-β1	1.717 ± 0.054	1.842 ± 0.053
0.1 µM MTX	2.227 ± 0.055	2.054 ± 0.243
1.0 µM MTX	2.107 ± 0.149	2.596 ± 0.223
5.0 mM TAA	2.056 ± 0.318	1.636 ± 0.292
15 mM TAA	*	1.086 ± 0.190

Figure 8: Measurement of cytokine levels at Tx7 and Tx14 (n = 5) showed treatment- and time-dependent differences in immunomodulatory and chemotactic cytokines. **(A)** IL-6 regulates acute phase response proteins in response to injury and was significantly increased at Tx7 for 1.0 µM MTX and both TAA treatment groups. **(B)** Monocyte chemotactic protein-1 (MCP-1), involved in facilitating macrophage/monocyte infiltration to perpetuate an adaptive response to continued insult, increased at Tx14 for MTX and TAA treatment. **(C)** Up-regulation of two fibrosis-associated genes. The levels of fibrogenic markers α-smooth muscle actin (*ACTA2*) and collagen, type 1, α1 (*COL1A1*) were measured using RNA isolated from whole tissue constructs at treatment day 14. Values are represented as fold-change relative to vehicle control (mean ± SD, N=2); shaded values denote a fold-change greater than 2. Treatment-induced induction of these genes suggests active fibrogenic processes and provide evidence to support collagen deposition within the tissue constructs.

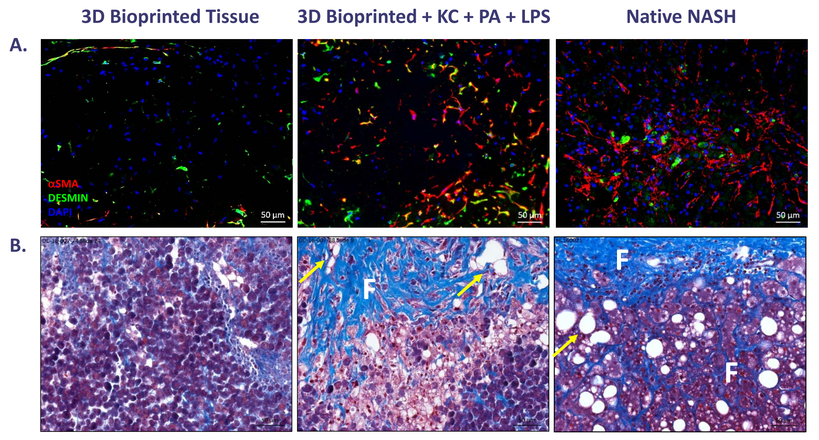

Figure 9: Progression of steatosis to inflammation with fibrosis can be observed following incorporation of Kupffer cells (KC) and treatment with palmitic acid (PA) in conjunction with lipoplysaccharide (LPS). **(A)** Increased activation of hepatic stellate cells (by α-SMA staining) is apparent, similar to native tissue samples. **(B)** Trichrome staining reveals increased fibrosis (F; regions of increased collage staining in blue) and steatosis (arrows), similar to native tissue samples.

Summary

- **Organovo's bioprinting platform enables the construction of 3D human tissue with complex architecture, sustained function and viability.**
- **ExVive™ Human Liver Tissue can recapitulate a variety of disease relevant phenotypes including steatosis, inflammation and fibrosis.**
- **ExVive™ Liver Tissue holds promise for the study of complex, chronic conditions such as NASH, enabling the discovery of novel therapeutics, biomarkers, and safety assessment of drugs in a disease-relevant background.**